Research article

polymers advanced technologies

Received: 18 October 2010, Revised: 24 January 2011, Accepted: 26 January 2011, Published online in Wiley Online Library: 29 March 2011

(wileyonlinelibrary.com) DOI: 10.1002/pat.1957

Diffusion energies of oxygen diffusing into polystyrene (PS)/poly (*N*-isopropylacrylamide) composites

Ö. Yargı[a], Ş. Ugur[a]* and Ö. Pekcan[b]

Diffusion coefficient of oxygen penetrating into polystyrene (PS) latex/poly (*N*-isopropylacrylamide) (PNIPAM) microgel composite films were measured using Fluorescence technique. Three different (5, 15, and 40 wt%) PS content films were prepared from PS/PNIPAM mixtures. Diffusivity of PS/PNIPAM composite films were studied by diffusionAAR_af1 measurements which were performed over the temperature range of 24–70°C. Pyrene was used as the fluorescent probe. The diffusion coefficients (*D*) of oxygen were determined using the Stern–Volmer fluorescence quenching method combined with Fickian transport and were computed as a function of temperature for each PS content film. The results showed that *D* values were strongly dependent on both temperature and PS content in the film. Diffusion energies were measured and found to be dependent on the composition of the composite films. **Copyright © 2011 John Wiley & Sons, Ltd.**

Keywords: latex; PS; PNIPAM; fluorescence; quenching; oxygen diffusion

INTRODUCTION

In last two decades, it has been well established that hydrogels play an important role in living systems and are of broad interest for a large variety of industrial products.[1,2] Hydrogels, as a type of biocompatible polymer, have wide applications in biological and medical fields.[3] These gels can be regarded as intermediates between solids and liquids, which exhibit a rather complex mixture of the properties of these limiting states. Thermosensitive systems like poly (*N*-isopropylacrylamide) (PNIPAM) and hydrogels have attracted much attention,[4] because the viscoelastic characteristics can be easily controlled by changing the temperature. In aqueous solution, PNIPAM exhibits a lower critical solution temperature (LCST) between 30 and 35°C that results in a reversible transformation from a hydrophilic polymer to one that is hydrophobic as the solution temperature is raised above the LCST. With an LCST close to normal body temperature, the thermosensitive nature of PNIPAM has resulted in a wide number of investigations for potential use in drug delivery systems. In thin-film geometry, such gels are of interest for applications such as thermosensitive surfaces, artificial pump and muscles, light modulation systems, and optical switches.

Large size PNIPAM gels have the disadvantage that the swelling and shrinking processes occur on a rather long time-scale. A recent trend in creating responsive, polymeric hydrogels is thus to decrease the size of the responsive units. In bulk systems, this has been achieved by synthesizing microgels[5–9] as colloidal particles with a cross-linked hydrophobic core and a cross-linked hydrophilic and responsive shell[10–13] or by exploiting the potential for self-assembly of amphiphilic block copolymers containing the responsive PNIPAM block. It is advantageous to use PNIPAM together with a hydrophobic block[14–17]. In most cases, polystyrene (PS) was chosen as the hydrophobic block.[14,16] Chemical crosslinking is often used when hydrogels must be insoluble in water and require mechanical strength for handling. Chemical crosslinking, however, is difficult to control in a melt fabrication process, and it is not reversible.

Composites based on hydrogels have shown many exciting properties. An actuation system based on sub-micrometer-sized silicon columns with a hydrogel layer was demonstrated to show humidity-responsive behavior.[18] As hydrogels are normally temperature-responsive polymers, such composites may also present useful temperature-sensitive properties. PNIPAM was chosen because it is one of the most popular and intensively studied hydrogels, and has found wide applications in many fields. It was reported that PNIPAM may have limited potential as a biomaterial[19,20] and PLGA/MI*x*-PNIPAM thermoresponsive dispersions can be used as an injectable highly porous biodegradable cell delivery system. Several investigations have incorporated PNIPAM into aqueous core–shell nanoparticles, for which diverse thermally responsive properties can be obtained.[21–23] Polymers have been extensively investigated for use in systems to modify the transmission of light or an attenuation of color with change in temperature. Many of the systems investigated are based on polymer-based gels that contain thermoresponsive dyes[24] or dispersed liquid crystalline phases.[25] Among these, best known are the thermotropic liquid

* *Correspondence to: Ş. Ugur, Department of Physics, Istanbul Technical University, Maslak 34469, Istanbul, Turkey.*
E-mail: saziye@itu.edu.tr

a *Ö. Yargı, Ş. Ugur*
Department of Physics, Istanbul Technical University, Maslak 34469, Istanbul, Turkey

b *Ö. Pekcan*
Kadir Has University, Cibali 34320, Istanbul, Turkey

 Copyright © 2011 John Wiley & Sons, Ltd.

crystalline compounds that can change transmissivity as they pass through a thermal transition from one phase to another. Liquid crystalline compounds often show thermochromic responses derived from the change in molecular order.[26] Acrylamide-based hydrogels have used the LCST to impart a thermotropic response, with the transition to the collapsed form attenuating transmission through light scattering.[27]

For many hydrogel applications, biocompatibility is also required and the material must also have high oxygen permeability, water sorption, and wettability.[28] Most of these properties are inter-related.[28,29] For example, oxygen permeability is largely related to water content and also influences biocompatibility. Oxygen is the one of the most important reactants to be considered in the diffusion phenomenon. The control of the diffusion of oxygen is of particular importance in polymer oxidative degradation, protective coatings, and in the design of polymeric membranes for separation processes in production of films for packing industry and in the developments of biocompatible materials.

For more than 50 years, polymer scientists have been interested in the influence of fillers on gas diffusion through polymer membrane.[30–34] Lu et al.[32] examined the influence of 10 nm diameter silica particles on oxygen diffusion in PDMS polymer film. A decrease was observed in oxygen diffusion coefficients, *D* with increasing silica content. This reduction in *D* was attributed to the tortuous path for diffusing gas molecules and reduced molecular mobility of polymer chains caused by the filler particles. Bharadwaj[33] also addressed the modeling of gas barrier properties in polymer-layered silicate nanocomposites based on a tortuosity argument. It was considered that the presence of filler introduces a tortuous path for a diffusing penetrant. The reduction of permeability arises from the longer diffusive path that the penetrants must travel in the presence of the layered silicate. Villaluenga et al.[34] investigated the permeability, diffusivity, and solubility of helium, oxygen, and nitrogen in the unfilled and filled polypropylene (PP) membranes with montmorillonite clay using X-ray diffraction, thermogravimetric analyzer, tensile testing, and differential scanning calorimetry. They found that the filled membranes exhibited lower gas permeability compared to the unfilled PP membrane and both diffusivity and solubility were reduced by the presence of fillers. This reduction was interpreted in terms of decrease in available free volume in the polymer providing less sorption sites for gas molecules.

Guillet[35] obtained values of diffusion coefficients of oxygen in different polymer matrix by luminescent quenching experiments. Fluorescence method has also been used for monitoring diffusion of small molecules in polymer films.[35,36] The diffusion coefficient of oxygen into Poly (methyl methacrylate) (PMMA) was determined by the quenching of phosphorescence of phenanthrene added into polymer.[37] Barker[38] has utilized the bleaching action of oxygen on color centers produced by electron beam irradiation of polycarbonate and PMMA by following optically the moving boundary. The quenching of fluorescence of naphthalene in PMMA was studied by oxygen in thin films after displacement of nitrogen atmosphere over the sample by oxygen.[39] In some of our earlier studies, we examined the effect of temperature[40] and MNaLB content[41] on the oxygen diffusion coefficient, *D*, in PS/MNaLB composite films using steady state fluorescence (SSF) technique. In these studies, we found that *D* values increased by increasing both temperature[40] and MNaLB content.[41]

In this work the diffusion behavior of oxygen into PS/PNIPAM composite films was studied depending on temperature and PS content. Three different sets of composite films were prepared from pyrene (P) labeled PS latex and PNIPAM microgel mixtures with 5, 15, and 40 wt% PS content drying at room temperature. SSF technique was used to study oxygen diffusion into these composite films over the temperature range of 24–70°C. The time drive mode of SSF spectrometer was employed to monitor the intensity change of excited P during oxygen penetration into composite films. A model was developed for low quenching efficiency to measure oxygen diffusion coefficient, *D*. This study has shown that addition of a hydrophobic PS particles to hydrophilic PNIPAM matrix results in a thermoresponsive dispersion. The PS/PNIPAM dispersions undergo phase separation upon heating and cause the formation of microvoids in the films which facilitates oxygen diffusion.

EXPERIMENTAL

PS latex particles

Pyrene labeled PS particles were produced via surfactant free emulsion polymerization process. The polymerization was carried out in a four-neck glass reactor equipped with a glass paddle agitator, condenser, and nitrogen inlet. The agitation rate was 300 rpm and the polymerization temperature was controlled at 70°C. Water (100 ml), styrene (5 g), and the 0.011 g of fluorescent 1-pyrenylmethylmethacrylate (PolyFluor 394) were first mixed in the polymerization reactor and when the temperature was constant (at 70°C), potassium peroxodisulfate (KPS) initiator (0.2 g) dissolved in small amount of water (2 ml) was introduced in order to induce styrene polymerization. The polymerization was conducted during 18 hr.[42] The synthesized latex particles are fairly monodisperse, having all very similar mean diameters (900 nm) and a $T_g = 105$°C.

Poly *N*-isopropylyacrylamide (PNIPAM)

Poly *N*-isopropylyacrylamide microgel particles were synthesized via precipitation polymerization process.[43,44] *N*- isopropylacrylamide (NIPAM) from Kodak was purified using a 60:40 (v/v) of hexane and toluene mixtures. Methylene bisacrylamide (MBA) from Aldrich was used as crosslinker monomer as received. The polymerization was performed using (1.2 g) NIPAM, (0.059 g) MBA, and (0.018 g) KPS as initiators. All the reactants were first dissolved in water and introduced in the polymerization reactor. The polymerization was conducted (in 50 ml deionised water) under nitrogen atmosphere and at 70°C. The polymerization reaction was carried out in 100 ml four-neck glass reactor equipped with a glass anchor-type agitator (200 rpm), condenser, and nitrogen inlet. The polymerization reaction was conducted during 16 hr. The final conversion was gravimetrically determined and found to be 98.5%. The mean diameter of synthesized PNIPAM particles is 320 nm and their T_g is 135°C.

Film preparation

PS/PNIPAM composite films were prepared by the casting method. Three different films with 5, 15, and 40 wt% PS content were prepared from the dispersion of PS latex/PNIPAM microgel by using the relation $W_{PS}(\text{wt}\%) = (W_{PS}/(W_{PS} + W_{PNIPAM})) \times 100$, where W_{PS} and W_{PNIPAM} are the weight of PNIPAM and PS latex,

Copyright © 2011 John Wiley & Sons, Ltd.

respectively. By placing the same number of drops on a glass plate with the size of $0.8 \times 2.5\,cm^2$ and allowing the water to evaporate, dry films were obtained. Film thickness was measured around 8 μm.

Steady state fluorescence technique

Composite films were placed in a round quartz tube filled with nitrogen, in Perkin Elmer Model LS-50 fluorescence spectrophotometer. Slit widths were kept at 8 nm. Experiments were carried out below T_g of both PS and PNIPAM polymers, in the 24–70°C temperature range. A thermistor-based digital temperature probe was used to monitor temperatures. The temperature in the chamber was observed to remain constant within ±2°C during the course of diffusion measurements. In all experiments, P was excited at 345 nm and the intensity at the emission maximum (395 nm) was used for the P intensity (I) measurements. I was monitored against time at different temperatures for each PS content composite film after the quartz tube was open to the air for O_2 diffusion experiments by using time-drive mode of spectrophotometer. Since the diffusion measurements required that oxygen permeate only one surface of the film, to further ensure that lateral diffusion did not affect results, a small region in the center of the films was masked off for measurement using black tape on the opposite side of the window from the samples.

THEORETICAL CONSIDERATIONS

Stern–Volmer kinetics

When samples containing fluorescent probes are exposed to air or their solutions saturated with oxygen, the fluorescence intensity of the samples decreases and the rate of fluorescence decay increases due to oxygen quenching of the probe's excited state. The mechanism of quenching involves a sequence of spin-allowed internal conversion processes which takes place within a weakly associated encounter complex between probe and oxygen. The product is either a singlet ground state or an excited triplet species.[45] Data generated from oxygen quenching studies on small molecules in homogeneous solution are usually analyzed using the Stern–Volmer relation, provided that the oxygen concentration $[O_2]$ is not too high.[46]

Stern–Volmer Kinetics applies broadly to variations of quantum yields of photophysical processes such as fluorescence, phosphoresce, or photochemical reactions with the concentration of a given reagent which may be a substrate or a quencher. In the simplest case, a plot of fluorescence intensity versus concentration of quencher, $[Q]$ is linear obeying the following equation[46]

$$\frac{I_0}{I} = 1 + k_q \tau_0 [O_2] \tag{1}$$

Here k_q is the quenching rate constant, τ_0 the lifetime of the fluorescence probe, Q the quencher concentration, and I_0 is the fluorescence intensity for zero quencher content. This relation is called Stern–Volmer Equation.

This equation requires that the decay of fluorescence is exponential and, that quenching interactions occur with a unique rateconstant k_q. From the slope of a plot of I_0/I versus $[O_2]$, k_q can be determined provided that τ_0 is known. Diffusion coefficients related to the quenching events can be calculated from the time-independent Smoluchowski–Einstein[46] equation, $k_0 = 4\pi N_A(D_P + D_q)/1000$. Here, k_0 is the diffusion-controlled bimolecular rate constant and is related to the bimolecular quenching rate constant, k_q as:

$$k_q = pk_0 = \frac{4\pi N_A (D_P + D_q) pR}{1000} \tag{2}$$

where D_P and D_q are diffusion coefficients of the excited probe and quencher, respectively, p the quenching probability per collision, R the sum of the collision radii ($R_P + R_q$), and N_A is the Avogadro number. Equations (1) and (2) can also be applied to the case of quenching of polymer-bound excited states in glass as long as the fluorescence decay is exponential and k_q is a unique constant. A simplifying factor in the interpretation of k_q is the general assumption that $D_P << D_q$ when the probe is covalently attached to a polymer. For quenchers as small as molecular oxygen, this assumption is reasonable. On the time-scale of fluorescence the overall translational diffusion coefficient of the polymer coil is usually not important; the relevant diffusion coefficient is that for motion of individual chain segments.

Fickian diffusion

Fick's second law of diffusion was used to model diffusion phenomena in plane sheet. The following equation is obtained by assuming a constant diffusion coefficient, for concentration changes in time[47]

$$\frac{C}{C_0} = \frac{x}{d} + \frac{2}{\pi}\sum_{n=1}^{\infty} \frac{\cos n\pi}{n} \sin\frac{n\pi x}{d} \exp\left(-\frac{Dn^2\pi^2 t}{d^2}\right) \tag{3}$$

where d is the thickness of the slab, D the diffusion coefficient of the diffusant, and C_0 and C are the concentration of the diffusant at time zero and t, respectively. x corresponds to the distance at which C is measured. We can replace the concentration terms directly with the amount of diffusant, M by using the following relation:

$$M = \int_v C dV \tag{4}$$

when Eqn (4) is considered for a volume element in the plane sheet and substituted in Eqn (3), the following solution is obtained[47]:

$$\frac{M_t}{M_\infty} = 1 - \frac{8}{\pi^2}\sum_{n=0}^{\infty} \frac{1}{(2n+1)^2} \exp\left(-\frac{D(2n+1)^2\pi^2 t}{d^2}\right) \tag{5}$$

where M_t and M_∞ represent the amounts of diffusant entering the plane sheet at time t and infinity, respectively.

RESULTS AND DISCUSSION

Oxygen diffusion

Figure 1 presents normalized pyrene intensity, I_P curves as a function of time for the 15 wt% PS content film exposed to oxygen at elevated temperatures. The emission intensity decreased with time as oxygen diffused through the planar film and reached a plateau for all temperatures when the films were saturated. It has to be noted that this saturation process is completed at shorter times for higher temperatures showing

Copyright © 2011 John Wiley & Sons, Ltd.

polymers advanced technologies

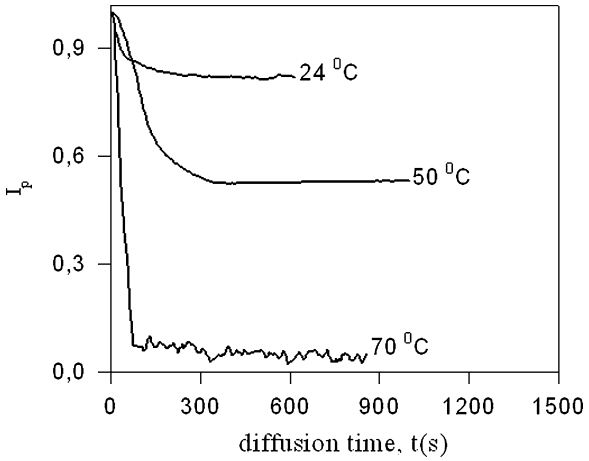


Figure 1. The time behavior of the pyrene, P, fluorescence intensity, *I*, during oxygen diffusion into the 15 wt% PS content film at various temperatures. Numbers on each curves indicate the temperature.

rapid diffusion of O_2 molecules. In addition, it is seen that at higher temperatures the rate of decrease in intensity is much higher predicting the more rapid quenching of excited pyrene molecules by O_2 molecules, diffused into the films. The curves reached their equilibrium values almost in the same fashion, as oxygen diffused through and equilibrated in the film. To interpret this observation Eqn (2) can be expanded in a series for low quenching efficiency, i.e.$\tau_0 k_q[Q] << 1$), which leads to

$$I \approx I_0\left(1-\tau_0 k_q[Q]\right) \tag{6}$$

In order to interpret the above findings Eqn (6) can be employed in the following manner; P molecules are quenched during diffusion into the films, in the volume which is occupied by O_2 molecules at time, *t*. Then P intensity at time *t* can be represented by the volume integration of Eqn (6) by replacing *Q* with O_2 as

$$I_t = \frac{\int I dv}{\int dv} = I_0 - \frac{k_q \tau_0 I_0}{V}\int dv[O_2] \tag{7}$$

where *dv* and *V* are the differential and total volume of the film as shown in Fig. 2. In Fig. 2, oxygen diffusion into the film is presented at different time steps, where pyrene quenching take place at $t > 0$ and levels off at $t = \infty$. Performing the integration the following relation is obtained

$$I_t = I_0\left(1-k_q\frac{\tau_0}{V}O_2(t)\right) \tag{8}$$

where $O_2(t) = \int dv[O_2]$ is the amount of oxygen molecules diffused into the film at time *t*. Here $O_2(t)$ corresponds to M_t in Eqn (5). Combining Eqn (5) for oxygen with Eqn (8) the following useful relation is obtained to interpret the diffusion curves in Fig. 1

$$\frac{I_t}{I_0} = A + \frac{8C}{\pi^2}\exp\left(-\frac{D\pi^2 t}{d^2}\right) \tag{9}$$

where *d* is the film thickness, *D* is the oxygen diffusion coefficient, $C = \frac{k_q \tau_0 O_2(\infty)}{V}$ and $A = 1-C$. Here $O_2(\infty)$ is the amount of oxygen molecules diffused into the film at time infinity. The logarithmic form of Eqn (9) can be written as follows:

$$\mathrm{Ln}\left(\frac{I_t}{I_0}-A\right) = \mathrm{Ln}\left(\frac{8C}{\pi^2}\right) - \frac{D\pi^2}{d^2}t \tag{10}$$

Figure 3a–c presents $\mathrm{Ln}(I_P/I_0 - A)$ versus diffusion time for the 15 wt% PS content film at various temperatures. Equation (10) is fitted to these data by the linear least square method and the oxygen diffusion coefficients, *D* at different temperatures were estimated from the slopes of the plots. Similar fittings were done for the other PS content films and *D* values were obtained at different temperatures, and are listed in Table 1. The average *D* values were determined from three or five measurements on different samples in each case. *D* values versus temperatures are also plotted for three PS content films in Fig. 4a where it is seen that *D* coefficients are strongly dependent on both temperature and PS fraction in the film. It is important to note that *D* increases with increase in temperature as expected for all composite films except for the 40 wt% PS content sample. When Table 1 and Fig. 4a are evaluated the following conclusions can be deduced: (i) diffusion is faster when the temperature is increased due to the

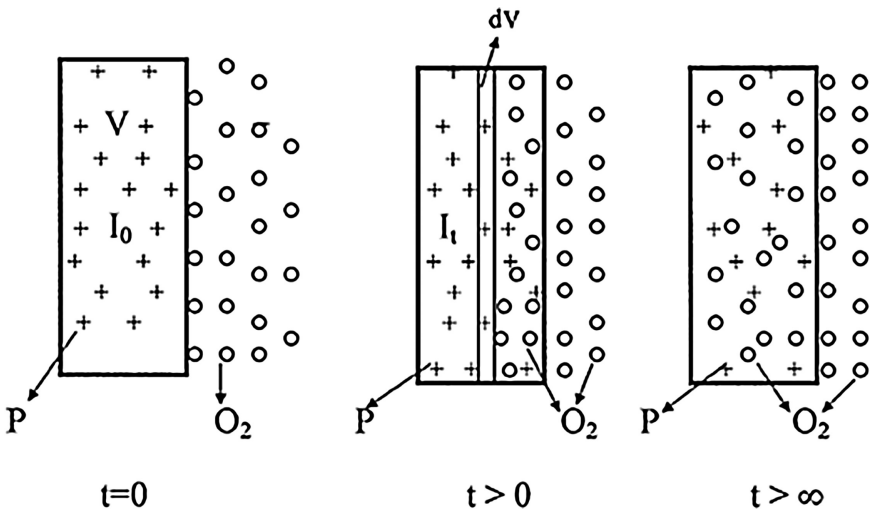


Figure 2. Cartoon representation of oxygen diffusion into the film at elevated time intervals.

 Copyright © 2011 John Wiley & Sons, Ltd.

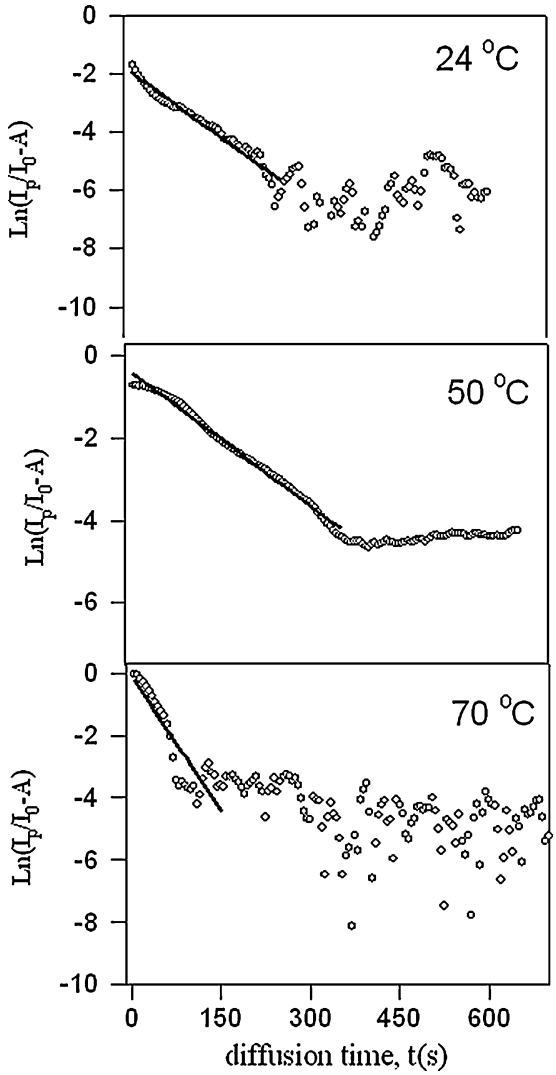


Figure 3. Logarithmic plot of the data in Fig. 1 according to Eqn (10) in the text. The slopes of the curves produced diffusion coefficients, *D*. Numbers on each curve shows the temperature.

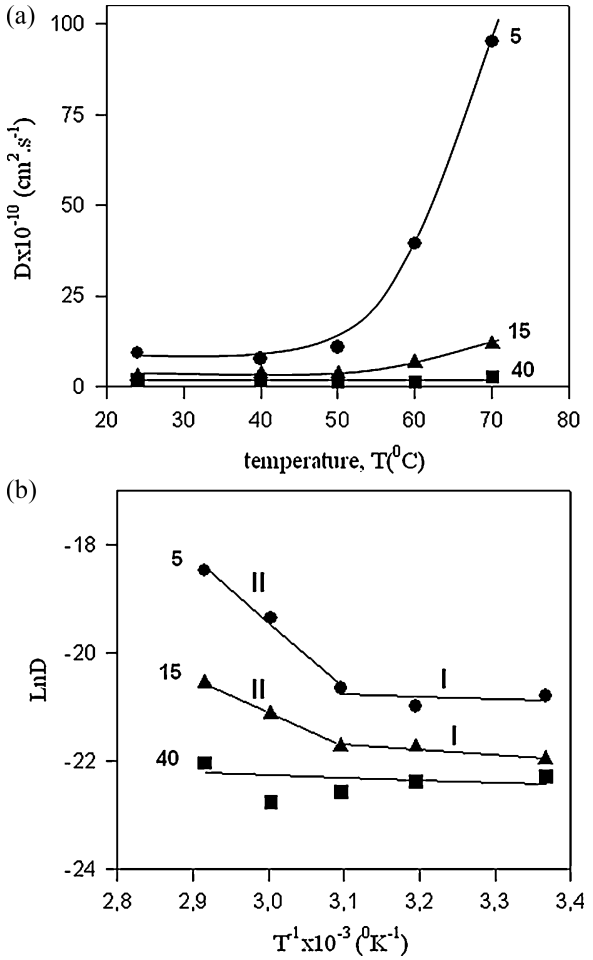


Figure 4. Plot of the (a) diffusion coefficients, *D* versus temperatures, *T* and (b) $\mathrm{Ln}(D) - T^{-1}$ for the 5, 15, and 40 wt% PS content films, respectively. ΔE_D values are obtained from the slopes of the straight lines for each PS content film.

Brownian motion of O_2 molecules in the composite film. (ii) Addition of 5 and 15 wt% PS in PNIPAM matrix creates a large fraction of microvoids inside the films. In our previous work inclusion of low percent of PS in PNIPAM presented lattice heterogeneities which caused a decrease in the transmitted light intensity around the 50°C annealing temperature.[48] Most probably these voids accelerate oxygen diffusion as temperature is increased. (iii) In samples with high percentage of PNIPAM (95 and 85 wt%) oxygen diffusion process can be accomplished in two stages. At first stage, below 50°C only a slight increase is seen in *D* values. At the second stage, above 50°C, *D* values increase more rapidly.

Table 1. Experimentally observed diffusion coefficients

	$D \times 10^{-10}$ ($\mathrm{cm}^2 \cdot \mathrm{s}^{-1}$)		
T (°C)	5	15	40
24	9.3 ± 0.5	2.9 ± 0.5	2.1 ± 0.1
40	7.7 ± 0.07	3.7 ± 0.2	1.9 ± 0.01
50	10.8 ± 0.5	3.7 ± 0.1	1.6 ± 0.02
60	39.5 ± 0.4	6.7 ± 0.2	1.3 ± 0.2
70	95.2 ± 2.4	11.8 ± 0.3	2.7 ± 0.1

Analysis using photon transmission technique[48] showed that doping of PNIPAM matrix with PS particles causes a minima in transmitted light intensity curves around 50°C. The decrease in transmitted light intensity, as measured by the reduction in transmittance at 500 nm, is a reversible process[48] with changes in temperature. As the temperature is increased above 50°C, there is a rapid drop in transmittance until 70–81°C depending on PS content in the film. Neither PNIPAM nor PS has a significant absorption at the 500 nm wavelength. The pyrene dye does absorb at 345 nm, but it is not temperature sensitive in this range. So, the change in transmittance is only dependent on the physical changes of the films and particle sizes. This decrease is due to the phase separation process between PNIPAM and PS particles resulting in increased light scattering. Therefore, the variation of *D* with respect to temperature in low PS content films can be explained with the presence of microvoids. AFM graphs for 5 wt% PS content film in Fig. 5 before and after heating also

Copyright © 2011 John Wiley & Sons, Ltd.

polymers advanced technologies

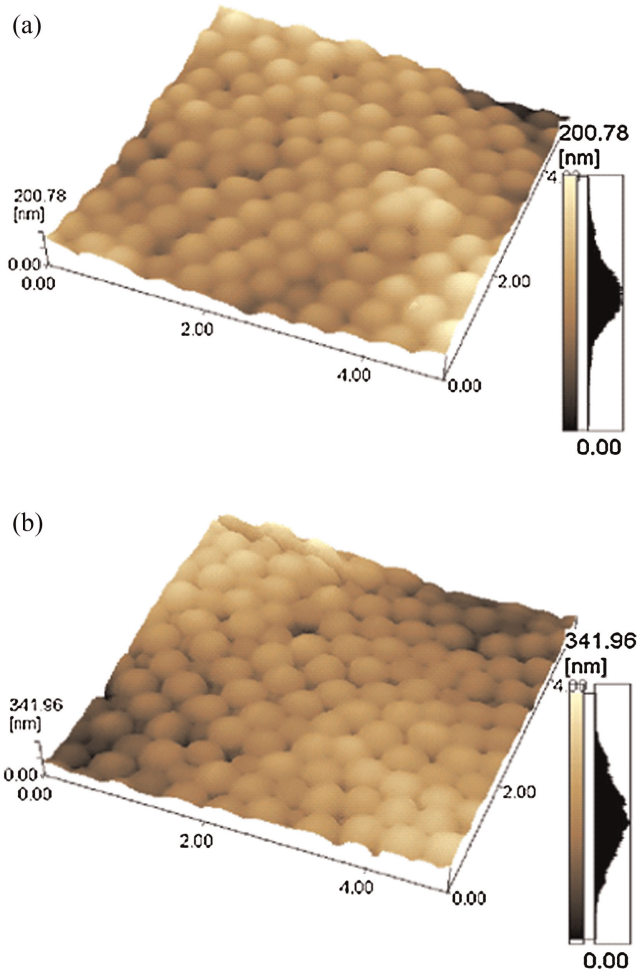


Figure 5. AFM images of PNIPAM film doped with 5 wt% PS; (a) before and (b) after the heat treatment.

confirm the above picture. It can be seen that there is a very high proportion of pores present. However, only a slight increase is seen in D values of 40 wt% PS content film with respect to temperature where no lattice heterogeneities were detected.[48] In other words 40 wt% PS content film possesses no microvoids, resulting no variation of D values with respect to temperature.

It is known that addition of filler into polymer films above a critical percentage creates voids[49,50] in the polymer matrix. Ponomarev and Gouterman[49] have reported that the addition of high amounts of titanium oxide (TiO_2) in PSP film cause the presence of a large fraction of microvoids inside the films. As a result, air can diffuse very rapidly to the inside of the coating through these voids. Kneas Kristi et. al.[50] studied the effect of silica (S) on diffusion coefficients, D of oxygen for pTMSMMA films. They found 2-fold decrease in D with increasing amounts of silica. They explained this decrease as a result of the strong adsorption of oxygen onto the hydrophobic amorphous silica particles due to their large surface area which acts to trap the oxygen. On the other hand, oxygen diffusion coefficients obtained in this study ($10^{-10}\,cm^2 \cdot s^{-1}$) are in the same order of magnitude with those previously obtained for PMMA films[51] of different thicknesses (10–100 μm) and PS/MNaLB[40,41] composite films by using the same technique.

Table 2. Experimentally observed diffusion activation energies

	5		15		
W_{PS} (wt%)	II	I	II	I	40
ΔE_D (kJ · mol^{-1})	100.3	3.05	53.4	7.9	3.7

Diffusion energies

It has been well established that the transport of gases through the membranes can be described as thermally activated process that obeys the Arrhenius behavior. In our case we take this advantage and write the temperature dependence of diffusion D coefficient as follows;

$$D = D_0 \exp\left(\frac{-\Delta E_D}{k_B T}\right) \tag{11}$$

Here k_B is the Boltzmann constant, D_0 is pre-exponential factor, and ΔE_D is the energy associated with the oxygen diffusion which can be determined from the logarithmic plots of the D coefficient against the reciprocal of the absolute temperature. In Fig. 4b, Ln(D) is plotted versus 1000/T for the different PS fraction. The value of energy associated with oxygen diffusion (ΔE_D) for different PS fractions were calculated from the slope of these plots fitting the data in Fig. 4b to the Eqn (11) by a least square fit. The results are given in Table 2 where it is seen that for 5 and 15 wt% PS content films, oxygen diffusion occurs in two stages with low and high energies. In fact, in 5 wt% PS content film O_2 gains larger energy during diffusion than the others, due to the large number of microvoids in the PNIPAM lattice. It is also seen from Fig. 4b that above 50°C energies are much larger than below 50°C. On the other hand, in 40 wt% PS content film the energy of O_2 is very low due to the slight variation of D with respect to temperature, i.e. due to the absence of microvoids in PNIPAM lattice.

CONCLUSION

The diffusion of oxygen into PS-PNIPAM composite films was studied at elevated temperatures for three different PS contents using fluorescence quenching method. The oxygen diffusion coefficients and related activation energies in these composite films were determined and compared. The results showed that diffusion of oxygen was accelerated by both increase in PNIPAM fraction and temperature. The high diffusion rate of oxygen in the composite is attributed to the formation of microvoids (pores) in the film which facilitates oxygen diffusion. The increase in the energy associated with the oxygen diffusion process (ΔE_D) is observed with increase in PNIPAM fraction. In conclusion, this work has shown that simple SSF technique can be used to measure the diffusion coefficient of oxygen molecules into composite films quite accurately.

REFERENCES

[1] Y. Hirokawa, T. Tanaka, *J. Chem. Phys.* **1984**, *81*, 6379.
[2] M. Shibayama, *Macromol. Chem. Phys.* **1998**, *199*, 1.

 Copyright © 2011 John Wiley & Sons, Ltd.

[3] J. Jagur-Grodzinski, *Polym. Adv. Technol.* **2006**, *17*, 395.
[4] M. Shibayama, T. Tanaka, C. C. Han, *J. Chem. Phys.* **1992**, *97*, 6829.
[5] M. Kratz, W. Eimer, B. Bunsenges, *Phys. Chem.* **1998**, *102*, 848.
[6] K. Kratz, T. Hellweg, W. Eimer, B. Bunsenges, *Phys. Chem.* **1998**, *102*, 1603.
[7] K. S. Oh, J. S. Oh, H. S. Choi, Y. C. Bae, *Macromolecules* **1998**, *31*, 7328.
[8] N. Dingenouts, C. Nordhausen, M. Ballauff, B. Bunsenges, *Phys. Chem.* **1998**, *102*, 1594.
[9] R. Pelton, *Adv. Colloid Interface Sci.* **2000**, *85*, 1.
[10] N. Dingenouts, C. Norhausen, M. Ballauff, *Macromolecules* **1998**, *31*, 8912.
[11] J.-H. Kim, M. Ballauff, *Colloid Polym. Sci.* **1999**, *277*, 1210.
[12] T. Hellweg, C. D. Dewhurst, W. Eimer, K. Kratz, *Langmuir* **2004**, *20*, 4330.
[13] M. Anderson, S. Hietala, H. Tenhu, S. L. Maunu, *Colloid Polym. Sci.* **2006**, *284*, 1255.
[14] M. Nuopponen, J. Ojala, H. Tenhu, *Polymer* **2004**, *45*, 3643.
[15] M. Mertoglu, S. Garnier, A. Laschewsky, K. Skrabania, J. Storsberg, *Polymer* **2005**, *46*, 7726.
[16] W. Zhang, X. Zhou, H. Li, Y. Fang, G. Zhang, *Macromolecules* **2005**, *38*, 909.
[17] A. Nykänen, M. Nuopponen, A. Laukkanen, S.-P. Hirvonen, M. Rytelä, O. Turunen, H. Tenhu, R. Mezzenga, O. Ikkala, J. Ruokolainen, *Macromolecules* **2007**, *40*, 5827.
[18] A. Sidorenko, T. Krupenkin, A. Taylor, P. Fratz, J. Aizenberg, *Science* **2007**, *315*, 487.
[19] H. Tanii, K. Hashimoto, *Toxicol. Lett.* **1991**, *58*, 209.
[20] I. Vyas, H. E. Lowndes, R. D. Howland, *Neurotoxicology* **1985**, *6*, 123.
[21] K. Makino, S. Yamamoto, K. Fujimoto, H. Kawaguchi, H. Ohshima, *J. Colloid Interface Sci.* **1994**, *166*, 251.
[22] C. Yi, Z. Xu, *J. Appl. Polym. Sci.* **2005**, *96*, 824.
[23] C.-L. Lin, W.-Y. Chiu, C.-F. Lee, *Polymer* **2005**, *46*, 10092.
[24] W. Y. Chung, S. M. Lee, S. M. Koo, D. H. Suh, *J. Appl. Polym. Sci.* **2003**, *91*, 890.
[25] B. Bahadur, *Liquid Crystal: Applications and Uses*, Vol. 3, World Scientific, Singapore, **1992**.
[26] D. J. Farina, J. M. Hacker, R. J. Moffat, J. K. Eaton, *Exp. Therm. Fluid Sci.* **1994**, *9*, 1.
[27] A. Seeboth, J. Schneider, A. H. Patzak, *Sol. Energy Mater. Sol. Cells* **2003**, *60*, 263.
[28] H. Zhang, T. E. Hogen-Esch, F. Boschet, A. Margaillian, *Polym. Prepr. (Am. Chem. Soc., Div. Polym. Chem.)* **1996**, *37*, 731.
[29] Y. C. Lai, A. C. Willson, G. Zantos, L. Òcontact, *Kirk-Othmer Encyclopedia of Chemical Technology*, 4th Edition, 7, Wiley, New York, **1993**, 192.
[30] R. M. Barrer, *Diffusion in Polymers*. (Eds. J. Crank, G. S. Park), Academic Press, New York, **1968**, 164–217.
[31] G. Gorrasi, M. Tortora, V. Vittoria, D. Kaempfer, R. Mülhaupt, *Polymer* **2003**, *44*, 3679.
[32] X. Lu, I. Manners, M. A. Winnik, *Macromolecules* **2001**, *34*, 1917.
[33] R. K. Bharadwaj, *Macromolecules* **2001**, *34*, 9189.
[34] J. P. Villaluenga, M. Khayet, M. A. Lopez-Manchado, J. L. Valentin, B. Seoane, J. I. Mengual, *Eur. Polym. J.* **2007**, *43*(4), 1132.
[35] J. E. Guillet, *Photophysical and photochemical tools in polymer science*. (Ed. M. A. Winnik), Reidel Publishing, Dordrecht, The Netherlands, **1986**, 467.
[36] J. E. Guillet, *Polymer photophysics and photochemistry*. Cambridge University Press, Cambridge, **1985**.
[37] G. Shaw, *Trans. Faraday Soc.* **1967**, *63*, 2181.
[38] R. E. Barker, *J. Polym. Sci.* **1962**, *58*, 553.
[39] J. R. MacCallum, A. L. Rudkin, *Eur. Polym. J.* **1978**, *14*, 655.
[40] Ş char203-
.*Uğur*, *Ö.Yarğı*, *Ö.Pekcan*, *Polym.Compos.***2010**, *31*, 77 − −782.
[41] Ş char203.*Uğur*, *Ö.Yarğı*, *Ö.Pekcan*, *Appl.ClaySci.***2009**, *43*, 447.
[42] Ş char203-
.*Uğur*, *A.Elaissari*, *Ö.Pekcan*, *J.ColloidInterfaceSci.***2003**, *263*, 674.
[43] F. Meunier, A. Elaissari, C. Pichot, *Polym. Adv. Technol.* **1995**, *6*, 489.
[44] F. Meunier, A. Elaissari, *Surfactant Science Series*, Vol. 115, Marcel Dekker, New York, **2003**, 117.
[45] J. B. Birks, "*Organic Molecular Photophysics*", Wiley-Interscience, New York, **1975**.
[46] S. A. Rice, "*Comprehensive Chemical Kinetics*". (Eds. C. H. Bamford, C. F. H. Tipper, R. G. Compton), Elsevier, Amsterdam, **1985**.
[47] J. Crank, "*The Mathematics of Diffusion*", Oxford University Press, London, **1970**.
[48] S. Ugur, O. Yargi, O. Pekcan, *Polym. Compos.* **2008**, *29*, 179.
[49] S. Ponomarev, M. Gouterman, presented at the 6th annual pressure sensitive paint workshop, Settle, WA, *Act.*, **1998**, 6.
[50] A. Kneas Kristi, J. N. Demas, B. Nguyen, A. Lockhart, W. Xu, B. A. DeGraff, *Anal. Chem.* **2002**, *74*, 1111.
[51] O. Pekcan, S. Ugur, *Polymer* **2000**, *41*, 7531.

Copyright © 2011 John Wiley & Sons, Ltd.